Asian Journal of Chemistry; Vol. 37, No. 5 (2025), 1229-1236

ASIAN JOURNAL OF CHEMISTRY

https://doi.org/10.14233/ajchem.2025.33465

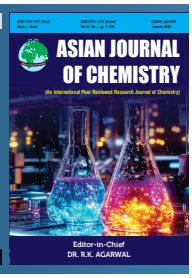

Eco-Friendly Synthesis, Characterization and Biological Activities of Silver Nanoparticles from *Terminalia chebula* Fruit

M. Sankar Kumar[1,2,*], Sailatha Ethirajulu[1] and Gunasekaran Sethu[3]

[1]Spectro Physics Research Laboratory, PG & Research Department of Physics, Pachaiyappa's College (Affliated to University of Madras), Chennai-600030, India
[2]Department of Physics, Rajalakshmi Engineering College, Thandalam, Chennai-602105, India
[3]SAIF, St. Peter's University of Higher Education and Research, Avadi, Chennai-600054, India

*Corresponding author: E-mail: sankarkumarm2012@gmail.com

Received: 2 February 2025; *Accepted*: 26 April 2025; *Published online*: 30 April 2025; AJC-21992

The current study involves of the synthesis and characterization of silver nanoparticles using a methanol extract of *Terminalia chebula* fruit as a reductive and stabilizing agent. The UV-visible peak of the obtained silver nanoparticles was visible at 470 nm. The presence of the hydroxyl and primary amines functional groups was identified with FT-IR analysis. According to SEM and EDAX images, the synthesized silver nanoparticles are primarily spherical and have a limited size distribution between 80 to 110 nm. The analysis of biosynthesized silver nanoparticles revealed the distinct peaks (signals), confirming the presence of silver metal. Among the tested bacteria, *Salmonella* sp. exhibited the least sensitivity to the green-synthesized silver nanoparticles, with a 4 mm inhibition zone, whereas higher inhibition zones were recorded for *Staphylococcus aureus* (6 mm), *Escherichia coli* (7 mm) and *Bacillus cereus* (6 mm). The biosynthesized silver nanoparticles exhibited a concentration-dependent enhancement in DPPH activity, with an average IC_{50} value of 794.07 µg/mL. The MTT assay was also employed to study anticancer effects of biosynthesized silver nanoparticles on human-origin cancer cell lines (HeP-2, Vero and MDAMB-231). When tested against HeP-2, Vero and MDAMB-231 cell lines, varying concentrations of the biosynthesized silver nanoparticles (TC-ME AgNPs) showed the morphological degeneration, cytotoxicity and damage. However, they were more effective against HeP-2 cells and MDAMB-231 cells. The findings suggest that silver nanoparticles, which could be useful in a variety of biological applications, can be produced efficiently from plant resources.

Keywords: *Terminalia chebula*, Medicinal plants, Silver nanoparticles, Antimicrobial activity, Anticancer activity.

INTRODUCTION

Nanotechnology centers around the creation, production and control of particles measuring between 1 and 100 nm [1]. In this range of size, individual atoms and the associated bulk material experience significant alterations in their chemical, physical, mechanical and biological properties [2]. It is due to their reduced size, particles which have higher surface area to volume ratios. Nanoparticles made from plant extract have gained significant interest lately attributable to their remarkable properties and good range of uses in the water treatment, pharmaceutical applications, agriculture and crop protection, optoelectronics, plasmonic and catalysis [3-8].

The "King of Medicine," *Terminalia chebula*, is prized for its potent antibacterial, antioxidant and anti-inflammatory qualities. It has been shown to be effective in treating infections, digestive problems and long-term illnesses including diabetes and heart disease [9,10]. There are few findings on the applications of *T. chebula* extracts for anticancer investigations [11,12], especially against numerous cell lines, despite the fact that they have previously been studied for their antibacterial and antioxidant properties. In this study, the silver nanoparticles was synthesized using an environmental friendly process and thoroughly assessed their effectiveness in biological activities, including cytotoxicity against the different cell lines *e.g.* HeP2 (laryngeal carcinoma), Vero (normal epithelial) and MDA-MB-231 (breast cancer).

EXPERIMENTAL

***Terminalia chebula* fruit extract preparation:** AR grade chemicals and solvents were procured from Sigma-Aldrich

Chemicals, USA and the fresh *T. chebula* fruits were obtained from the local market of Chennai city, India. In a sterilized and dried 500 mL Erlenmeyer flask, 25 g of finely chopped fruit was combined with 200 mL of methanol to obtain the fresh *T. chebula* fruit extract utilized for the reduction of Ag^+ ions to Ag^0. Before decanting, the mixture was chilled for 24 h at 2-8 ºC. After that, extract was passed through Whatman No. 1 filter paper and maintained at 4 ºC for subsequent procedures.

Phytochemical analysis: Following established biochemical procedures [13], the methanolic extract of *T. chebula* fruit was analyzed to detect the presence of phytochemicals such as coumarins, anthocyanins, quinones, carbohydrates, alkaloids, glycosides, saponins, starch, steroids, proteins, organic acids, phenols, terpenes, tannins, flavonoids, carotenoids, lignans, essential oils, lectins and glucosinolates.

Synthesis of silver nanoparticles: In brief, the methanol fruit extract *T. chebula* (10 mL) and silver nitrate solution (90 mL, 1.0 mmol) in water were mixed thoroughly and then centrifuged at 10,000 rpm for 10 min under refrigerated conditions (4 ºC). The obtained pellet was kept in storage for additional analysis [14]. Visually observable changes in reaction solution colour from colourless to brown indicate the formation of AgNPs during the reduction process [15-17].

Characterization: In the 300-800 nm range, the absorption spectrum characteristics of fruit extract and the metal content were investigated using a Perkin-Elmer Lambda-45 spectrophotometer. The FT-IR analysis was carried out with a Shimadzu 8400 S equipment at a resolution of 4 cm^{-1} within the spectral range of 4000-400 cm^{-1}. To assess the crystallinity and particle size of the silver nanoparticles, XRD analysis was carried out with Shimadzu Lab-X XRD-6000 system, utilizing Cu$K\alpha$ radiation (λ = 1.540 nm) at 20-30 kV and 30 mA for diffraction analysis. The scanning was conducted in continuous scan mode over a 20º to 90º range, with a scan rate of 0.24 sec per step. The morphology using SEM with EDAX analysis was analyzed using a SEM (JEOL JSM-6360, Japan) equipped with an EDX detector (EDS, EDAX Inc., Mahwah, NJ, USA).

Antibacterial activity: The antibacterial activity of biosynthesized silver nanoparticles was assessed using the disc-diffusion method [18]. Sterile discs were used and the sample placed in a Petri dish for 2 h in order to promote adequate absorption. After that, the produced discs were placed on MHA plates that had already been seeded with bacterial strains. Following an initial diffusion period of 1 h, the plates were incubated at 37 ºC for 24 h. Antibacterial activity was assessed by measuring the diameter of the inhibition zones (in mm) using a standard ruler. Ampicillin (10 µg/mL) was used as a reference antibiotic for comparison.

Antifungal activity: On Sabouraud Dextrose agar (SDA), the disc diffusion technique was used to assess the antifungal properties of biosynthesized silver nanoparticles. A sterile swab was used to distribute a fungal solution evenly across the surface of Petri plates after the SDA was poured and then allowed to solidify. Discs containing the sample and amphotericin B, the positive control, were put on the agar. The antifungal activity was next assessed by measuring the diameter of the inhibitory zones during a 24 h incubation period at 37 ºC [19].

DPPH radical scavenging assay: A slightly modified method was employed to evaluate the overall capacity of AgNPs to scavenge free radicals using the stable DPPH radical, which has maximum absorption at 515 nm [20-22]. To make the DPPH radical solution, 2.4 mg was dissolved in 100 mL of methanol. For the antioxidant experiment, 5 µL of extract was treated with 3.995 mL of DPPH solution. After thorough shaking, it was left at room temperature for 0.5 h in dark. A blank solution containing DPPH without any antioxidant was employed as control and the absorbance of the reaction mixture was measured by spectrophotometric measurement at 515 nm. The ability to scavenge the DPPH radical was calculated using the following formula:

$$\text{DPPH scavenged (\%)} = \frac{mn - ab}{mn} \times 100$$

where, mn is absorbance of blank at t = 0 min; ab is absorbance of the antioxidant at t = 30 min.

Superoxide dismutase assay (SOD): Superoxide dismutase in tissue and cancer cells was measured using the reported method [23]. The assay is based on the inhibition of nitro blue tetrazolium formation from NADH-phenazine methosulphate. The reaction commenced upon the addition of NADH. Anhydrous acetic acid was added at the 90 sec interval to terminate the reaction. The colour produced at the end of the reaction was measured at 520 nm using a spectrophotometer following extraction into an *n*-butanol layer.

Cell line cultures: Cell lines MDA-MB-231, Hep-2 and VERO were acquired from the King Institute of Preventive Medicine & Research, Chennai, India. Cell cultures were maintained at 37 ºC in MEM supplemented with 10% FBS, 100 U/mL penicillin and 100 µg/mL streptomycin to maintain cell growth. To promote the best possible cell growth, the incubation atmosphere was humidified with 5% CO_2.

***In vitro* cytotoxicity evaluation using MTT assay:** After being plated in 24-well plates, cells (1×10^5/well) were incubated at 37 ºC with 5% CO_2 until confluence. After adding the sample and incubating it for a full day, it was washed with either serum-free minimum essential medium (MEM) or phosphate-buffered saline (pH 7.4). Following 4 h of incubation with an MTT solution (100 µL/well, 5 mg/mL), 1 mL of DMSO was used to solubilize the formazan crystals. A UV spectrophotometer was used to detect absorbance at 570 nm and IC_{50} was graphically calculated.

RESULTS AND DISCUSSION

Phytochemical studies: The findings of a qualitative phytochemical screening of a *T. chebula* fruit methanol extract are shown in Table-1. The presence of coumarin, flavonoids, quinones, saponins, starch, steroids, acids, phenol, terpenes, tannins and glycosides were detected in synthesized AgNPs, which play a key role in ensuring the efficient of capping agent-mediated stabilization of nanoparticles, as confirmed by the FT-IR spectrum [24]. Several bioactive compounds present in the plant material were identified with the help of preliminary phytochemical investigation. Consequently, *T. chebula* fruit was selected for the synthesis of AgNPs to assess its antibacterial,

TABLE-1
PHYTOCHEMICAL RESULTS OF
METHANOL EXTRACT OF *T. chebula* FRUIT

S. No.	Phytocompounds	Results
1	Anthocyanine/batacyanine	Present
2	Coumarines	Present
3	Flavonoids	Present
4	Glycosides	Present
5	Phenols	Present
6	Quinones	Present
7	Tannins	Present
8	Terpenoids	Present
9	Steroids	Present
10	Saponins	Present
11	Alkaloids	Absent
12	Carbohydrates	Absent
13	Cardiac glycosides	Absent
14	Proteins	Absent
15	Starch	Absent
16	Alkaloids	Absent

antioxidant and anticancer properties, owing to the rich presence of phytochemicals in the fruit [25].

UV-visible spectral studies: The formation of silver nanoparticles (AgNPs) from the methanolic extract of *T. chebula* fruit was affirmed by UV-Vis spectral spectroscopy. In resonance with the light wave, the free electrons of AgNPs generate simultaneous electron vibrations, which induce surface plasmon resonance (SPR) absorption. The SPR band of AgNPs may be seen in Fig. 1 at 470 nm. With longer reaction times, the synthesis of nanoparticles increased quickly. A key factor in the formation of symmetrical nanoparticles is the extract concentration. It is assumed that the natural extract functions similarly to a biological reducing agent because metal nanoparticles are frequently created using chemical compounds by redox reaction.

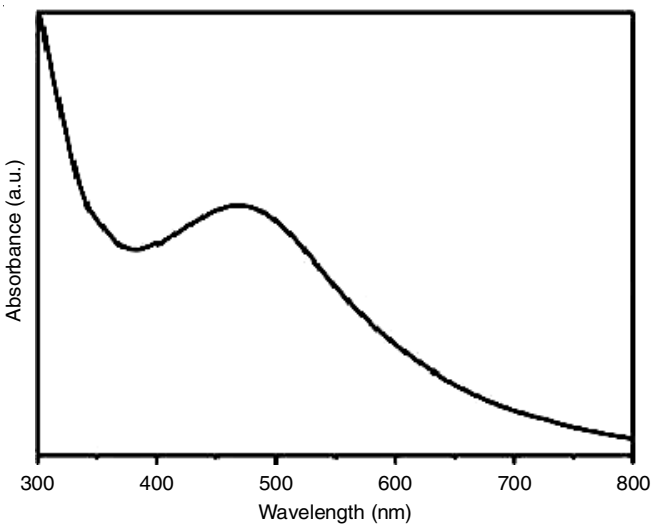

Fig. 1. UV-Vis spectrum of biosynthesized silver nanoparticles

FT-IR spectral studies: The biomolecules responsible for capping and stabilizing the silver nanoparticles synthesized from the methanol extract of *T. chebula* fruit were characterized through FT-IR analysis. In the FT-IR spectrum (Fig. 2), the peak at 1630.47 cm^{-1} represents the N-H bending of primary

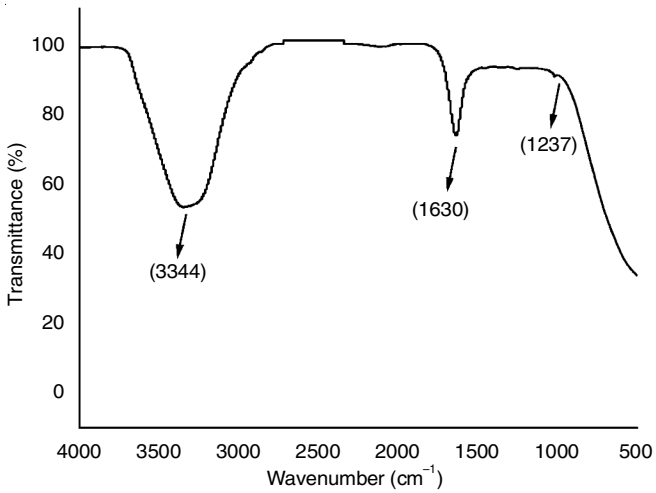

Fig. 2. FT-IR spectrum of biosynthesized silver nanoparticles

amines, whereas the O-H stretching vibration is detected at 3344.99 cm^{-1}. The C-N stretching due to the aromatic amine groups is linked to the peak at 1237.67 cm^{-1}. Native proteins, which have been demonstrated to interact with biosynthesized AgNPs without altering their secondary structure, are represented by the absorption band at 1630 cm^{-1}, which is stretching vibration of C=C bond [26,27]. The carbonyl groups present in proteins and amino acid residues appear to have a high propensity for interacting with metal ions, according to FT-IR spectrum. This indicates that proteins play a role in encapsulating AgNPs, preventing agglomeration and enhancing medium stability [28].

XRD studies: The formation of crystalline phases in the biosynthesized AgNPs was confirmed by powder XRD analysis. The XRD pattern (Fig. 3) shows the diffraction signal exhibited prominent peaks at 2θ values of 44.0º and 64.50º, which are in agreement with known phase patterns to the (200) and (220) reflecting the distinct planes of a face-centered cubic silver phase. As per standard JCPDS No. 04-0783, 2θ values 38.07º, 44.29º, 64.44º and 77.34º corresponding to 111, 200, 220 and 311 planes. Surface oxidation may occur if the XRD sample was prepared by drop-casting, slow drying, or storage before to analysis. Due to the significant surface reactivity of nanosized silver exposed to air and moisture, the XRD pattern displays

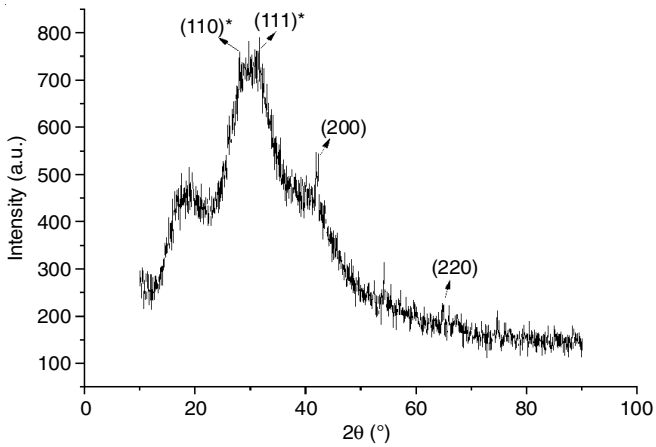

Fig. 3. XRD spectrum of *T. chebula* mediated silver nanoparticles

dominating the peaks related to Ag_2O rather than metallic Ag. It is commonly known that, especially at smaller particle sizes, silver nanoparticles frequently form a thin Ag_2O shell [29]. Nanoscale effects and mild surface oxidation are responsible for the observed decreased intensity and peak broadening, particularly around 28.5º and 32.2º [30-32].

SEM-EDX studies: The nanoparticles formed from silver metal were found to be spherical as confirmed from the SEM image and EDX results (Fig. 4). An optical absorption peak near 3 keV is commonly observed in metallic silver nanocrystals, attributed to surface plasmon resonance effects [17,33]. The spectrum indicates that the most prevalent element was silver (45.71%), which was followed by carbon (37.55%) and oxygen (12.86%).

Antibacterial activity: There are several ways in which silver nanoparticles (AgNPs) demonstrate antibacterial activity. They mostly stick to the membranes and cell walls of bacteria, damaging the structure and making the membranes more permeable, which eventually results in cell death. Furthermore, AgNPs produce reactive oxygen species (ROS) that cause oxidative stress in bacterial cells, such as hydrogen peroxide, superoxide anions and hydroxyl radicals [34-38]. To assess the antibacterial efficacy, the biosynthesized AgNPs were subjected to agar disc diffusion assay against a selection of pathogenic bacteria. The inhibition diameter shows the millimeter zone and AgNPs outperformed $AgNO_3$ solution and fruit extract in terms of activity (taken as controls) (Table-2). Higher AgNPs concentrations resulted in greater antibacterial activity. *Salmonella* spp. had the lowest zone of inhibition (1.8 mm), while *E. coli* exhibited the highest (7 mm). The results of this investigation are in line with earlier studies on the antibacterial properties of AgNPs [39]. The antibacterial effect may be ascribed to the exceptionally small AgNPs generated by the methanolic extract of *T. chebula* fruit extract, which possess a higher surface area than their smaller counterparts, facilitating enhanced contact with bacterial cell membranes and internal structures [40,41]. The SEM results obtained in this experiment corroborated this explanation.

Antioxidant efficacy: This study evaluated the antioxidant efficiency of phytomediated AgNPs and the methanolic extract of *T. chebula* fruit using the DPPH and FRAP assays, highlighting their free-radical quenching activity. The results indicate that the DPPH scavenging activity of both the extract and AgNPs increased with concentration, consistent with the reported in earlier studies [42]. The biosynthesized AgNPs had an inhibition percentage of 61.9% for AgNPs at the maximum concentration (Table-3). Moreover, the FRAP data revealed the fruit extract and AgNPs of 124.54% and 132.29%, respectively. The adsorption of bioactive components on the surface of the spherically shaped AgNPs contributed to their superior antioxidant potential compared to the extract [43]. This effect may also be attributed to the combined action of polyphenols as antioxidants and AgNPs as catalysts [44].

The SOD enzymatic activity of *T. chebula* fruit extract (36.21 ± 4.25) and biosynthesized AgNPs (41.49 ± 5.58) (U/mg protein) highlights the applications of AgNPs compared to the extract. At 1 µg/mL, treatment with AgNPs enhanced the enzymatic activity of superoxide dismutase in *Ricinus communis*; however, at 2 µg/mL, the SOD activity in plants treated with AgNPs decreased. SOD activity and the rate of lipid oxidative damage were found to be reveal an inverse association in the present investigation. According to the research, cellular comp-

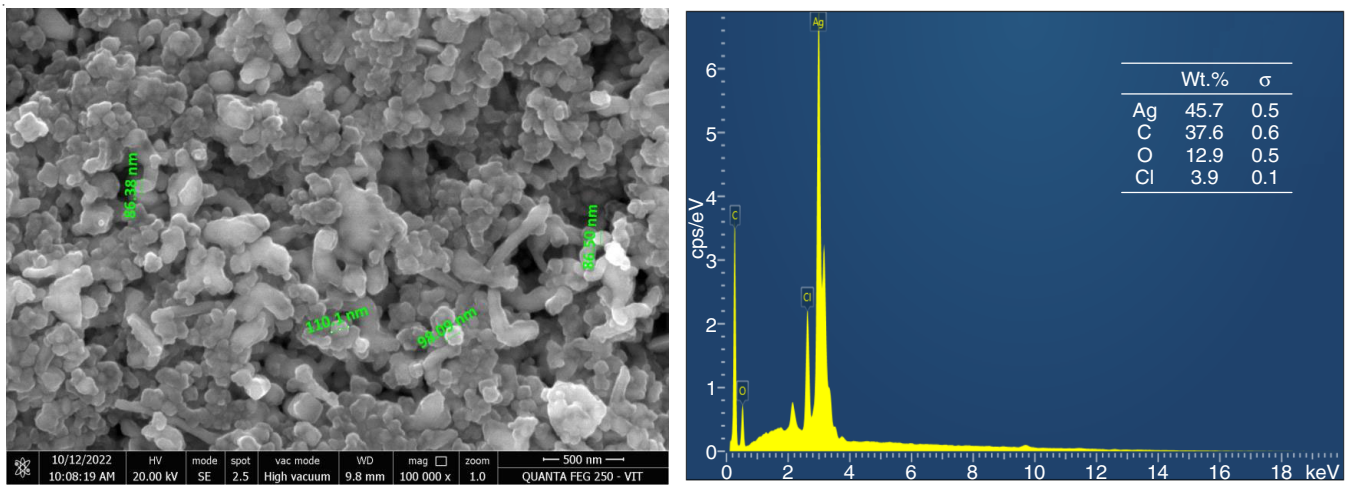

Fig. 4. SEM with EDX images of *T. chebula* mediated silver nanoparticles

TABLE-2
ANTIBACTERIAL EFFICACY DATA OF BIOSYNTHESIZED SILVER NANOPARTICLES

Organism	Antimicrobial inhibition zone measured (mm)			
	500 µg/mL	750 µg/mL	1000 µg/mL	Control
Staphylococcus aureus	4 mm	5 mm	6 mm	7 mm
Escherichia coli	4 mm	6 mm	7 mm	7 mm
Bacillus cereus	4 mm	5 mm	6 mm	8 mm
Salmonella sp.	1 mm	3 mm	4 mm	5 mm

TABLE-3
DOSE-DEPENDENT ANTIOXIDANT POTENTIAL OF SILVER NANOPARTICLES SYNTHESIZED FROM *T. chebula* FRUIT EXTRACT

Dose (µg/mL)	OD (517 nm)	DPPH radical inhibition (%)
200	0.825	10.96
400	0.592	35.72
600	0.501	45.60
800	0.431	53.20
1000	0.351	61.88
Standard	0.210	077.19

Blank OD = 0.921; IC_{50} = 794.07 µg/mL

onents may experience increased lipid peroxidation as an outcome of decreased SOD enzymatic activity, which could cause membrane damage [45,46].

Anticancer activity: The results from the *in vitro* cytotoxicity study conducted on the selected cell lines (Vero, Hep-2 and MDA-MB-231) are summarized, which suggest that biosynthesized AgNPs have anticancer properties (Table-4). The control group consisted of cells that were simply exposed to culture medium. Following a 24 h exposure, the cytotoxic effect of biosynthesized AgNPs against VERO, Hep-2 and MDA-MB-231 cell lines is shown in Figs. 5-7. All the investigated cell lines saw a concentration-dependent decline in cell survival after a 24 h incubation with biosynthesized AgNPs; the MDA-MB-231 cell line shown the highest sensitivity. The IC_{50} values for biosynthesized AgNPs were 46.98 µg/mL and (for 24 h of Hep-2 cell line incubation) as opposed to 46.66 µg/mL (for 24 h incubation of MDAMB-231cell line). The MDAMB-231 cell line was shown to be more responsive to biosynthesized AgNPs than the Vero cell line. The physical properties of biosynthesized AgNPs, including their size and shape, are intimately linked to their anticancer potential. Due to its higher surface-to-volume ratio, which encourages better

TABLE-4
IMPACT OF BIOSYNTHESIZED SILVER NANOPARTICLES ON DIFFERENT HUMAN CANCER CELL LINES

S. No.	Dose (µg/mL.)	Concentration ratio	Vero cell line		HeP_2 cell line		MDA-MB-231 cell line	
			Absorbance (O.D)	Cell viability (%)	Absorbance (O.D)	Cell viability (%)	Absorbance (O.D)	Cell viability (%)
1	1000	Neat	0.41	75.92	0.09	10.84	0.10	11.11
2	500	1:1	0.44	81.48	0.15	18.07	0.18	20.00
3	250	1:2	0.46	85.18	0.22	26.50	0.26	27.88
4	125	1:4	0.49	90.74	0.30	36.14	0.33	36.66
5	62.5	1:8	0.51	94.44	0.39	46.98	0.42	46.66
6	31.2	1:16	0.52	96.29	0.46	55.43	0.53	58.88
7	15.6	1:32	0.53	98.14	0.55	66.26	0.64	71.11
8	7.8	1:64	0.53	98.14	0.63	75.90	0.71	78.88
9	Cell control	–	0.54	100	0.83	100	0.90	100

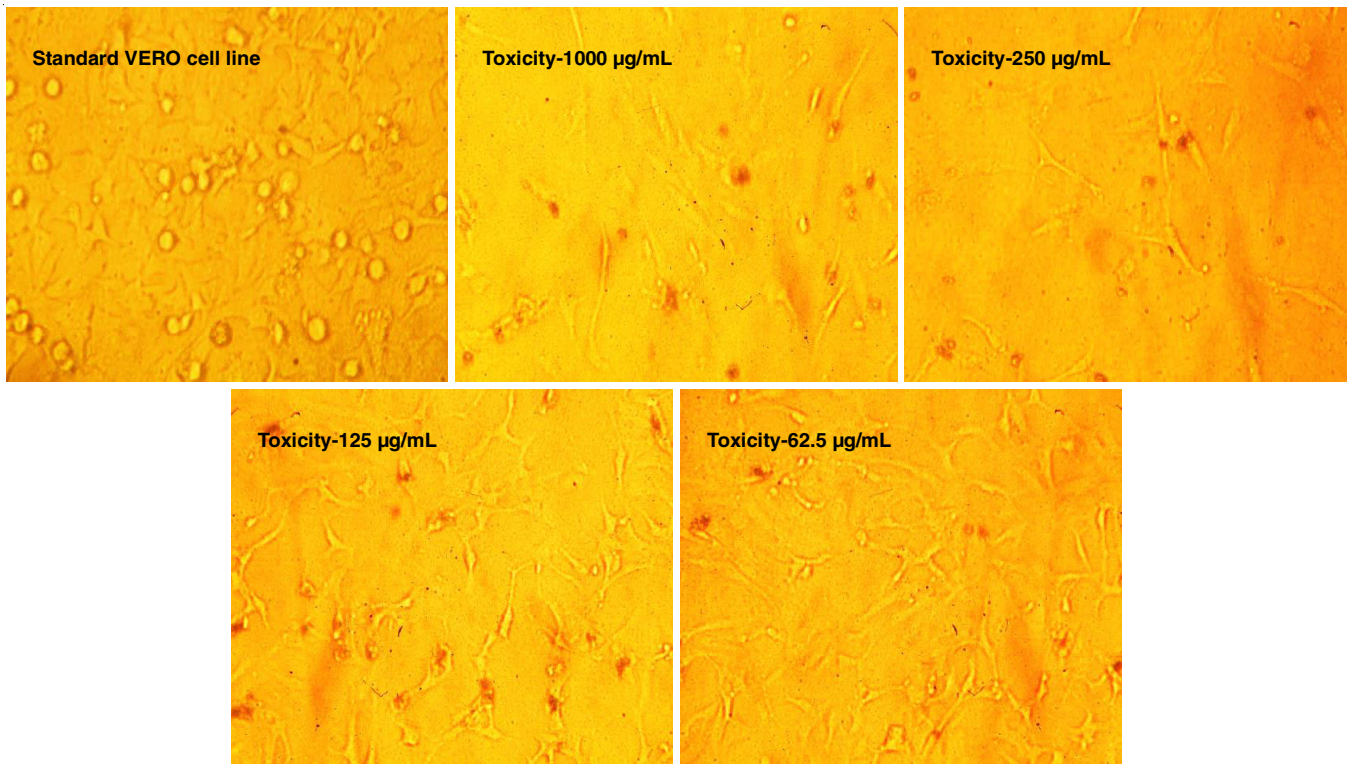

Fig. 5. Dose-dependent cytotoxic response of Vero cells to *T. chebula* mediated silver nanoparticles

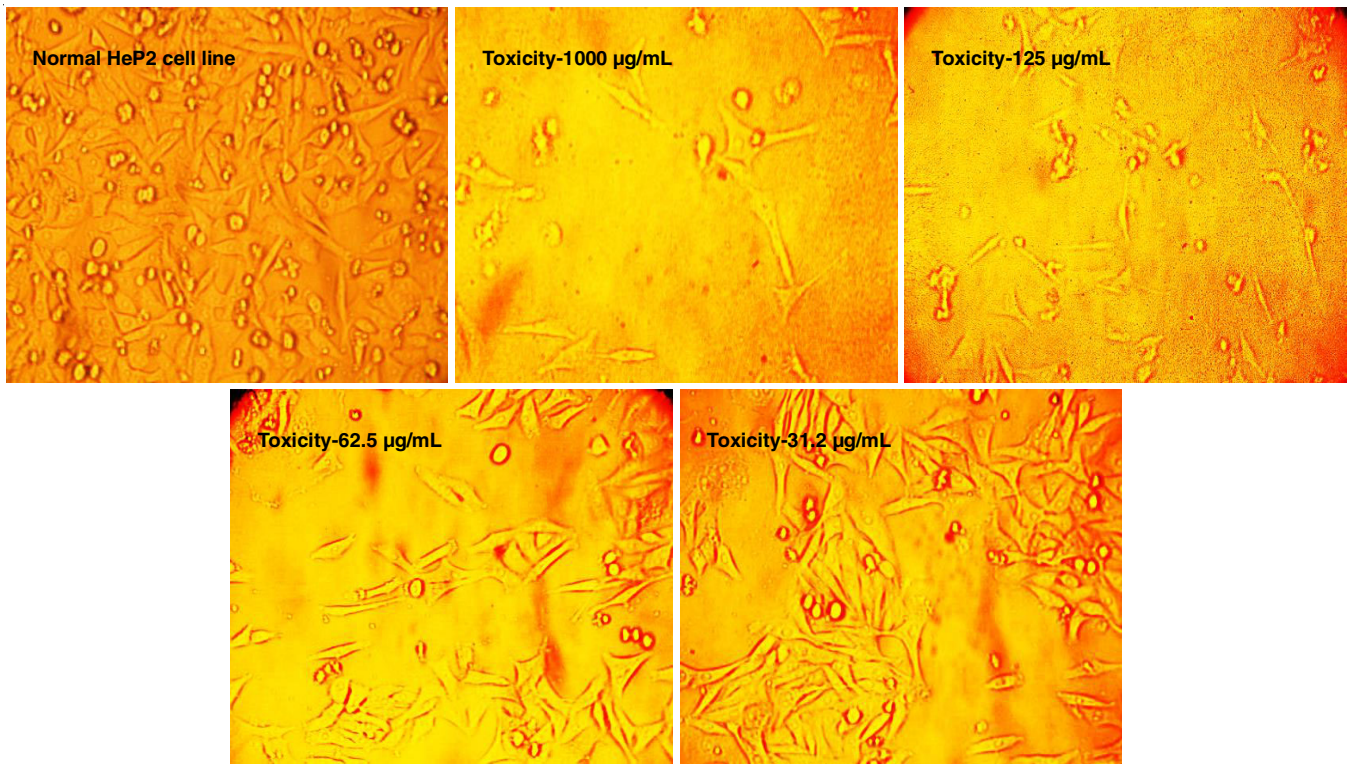

Fig. 6. Anticancer effect of *T. chebula* mediated silver nanoparticles on HeP2 cell line

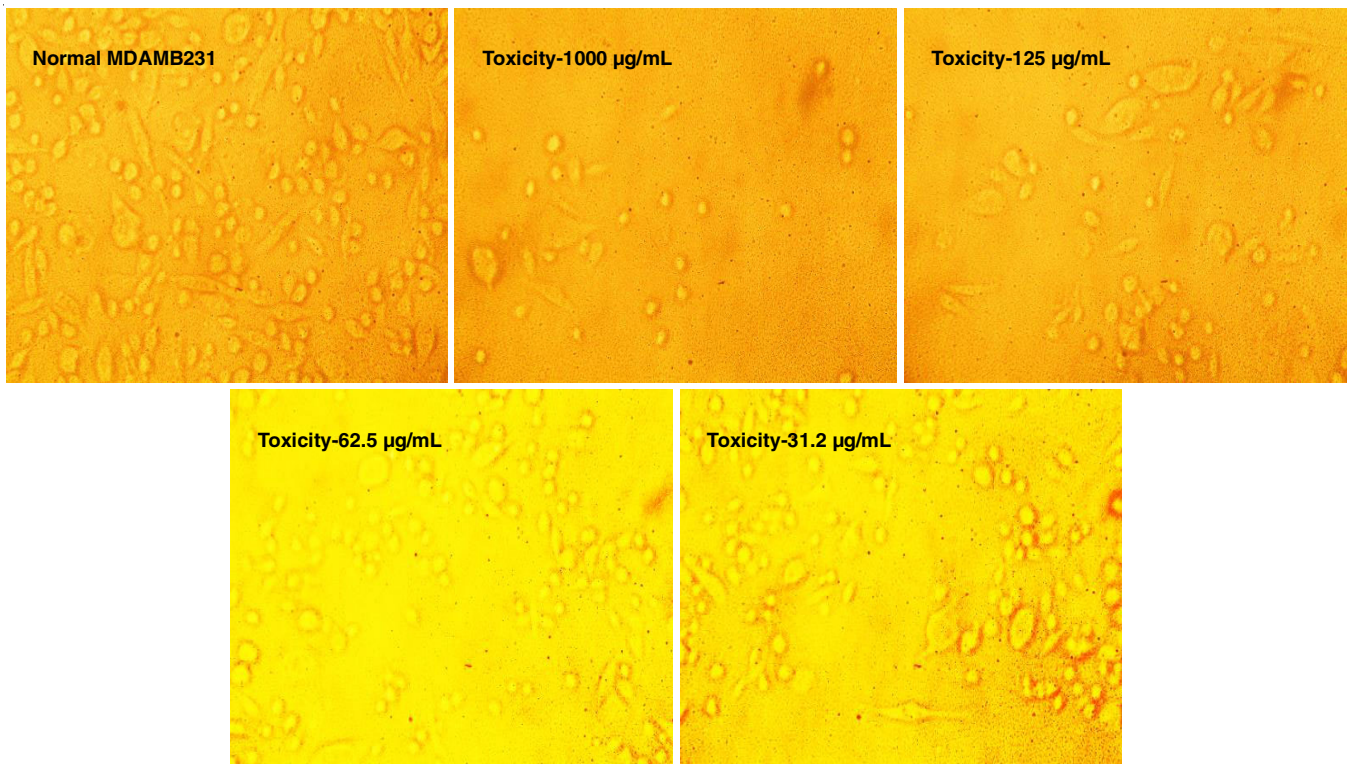

Fig. 7. Anticancer impact of *T. chebula* mediated silver nanoparticles on MDAMB231 cell line

cellular contact and uptake, spherical AgNPs have shown increased cytotoxicity when compared to other morphologies [47-50].

Silver nanoparticles with sizes between 10 and 100 nm are typically thought to be appropriate for anticancer applications due to their effective permeability, transport and cellular uptake properties [51]. Smaller sizes may be quickly released from normal arteries and cause harm to healthy cells. According to literature [52], AgNPs significantly affect the apoptosis of A549 lung cancer cells. The findings showed that AgNPs have anticancer properties and dose-dependently decrease the viability

of Hep-2 cancer cells. Thus, these findings seem encouraging considering the strong antibacterial and anticancer properties displayed by AgNPs.

Conclusion

This study examined the eco-friendly synthesis of silver nanoparticles using the methanol extract of *Terminalia chebula* fruit, followed by characterization and their biological activities. The silver anoparticles formation was validated by UV-visible spectroscopy, which showed an absorbance peak at about 470 nm. Functional groups like O-H and C-N were shown to be involved in the stabilization and capping of the nanoparticles by FT-IR analysis. A strong EDX signal featuring a significant peak near 3 keV indicates a significant silver presence (45.71%) and supports the formation of stable AgNPs, confirmed the effective synthesis of silver nanoparticles. Although the antioxidant IC_{50} values and antibacterial zone of inhibition indicated moderate performance, the biological assays showed that the synthesized AgNPs possess considerable antioxidant, antibacterial and anticancer activities. Notwithstanding certain drawbacks, including the lack of thorough mechanistic research and partial oxidation effects, this green synthesis method presents a viable and sustainable way to synthesize silver nanoparticles for use in pharmaceutical and biological applications.

ACKNOWLEDGEMENTS

For facilitating cell line studies and other biological analyses, the authors are thankful to Dr. Swaminathan, Director of Sasham Biological Pvt. Ltd., Chennai.

CONFLICT OF INTEREST

The authors declare that there is no conflict of interests regarding the publication of this article.

REFERENCES

1. A.M. Mahasneh, *Jordan J. Biol. Sci.*, **6**, 246 (2013); https://doi.org/10.12816/0001621
2. S.A. AlThabaiti, E.S. Aazam, Z. Khan and O. Bashir, *Spectrochim. Acta A Mol. Biomol. Spectrosc.*, **156**, 28 (2016); https://doi.org/10.1016/j.saa.2015.11.015
3. S. Muruganandam, G. Anbalagan and G. Murugadoss, *Appl. Nanosci.*, **5**, 245 (2015); https://doi.org/10.1007/s13204-014-0313-6
4. X.-M. Liu, Z.-B. Feng, F.-D. Zhang, S.-Q. Zhang and X.-S. He, *Agric. Sci. China*, **5**, 700 (2006); https://doi.org/10.1016/S1671-2927(06)60113-2
5. T.C. Prathna, S.K. Sharma and M. Kennedy, *Sep. Purif. Technol.*, **199**, 260 (2018); https://doi.org/10.1016/j.seppur.2018.01.061
6. A. Pugazhendhi, D. Prabakar, J.M. Jacob, I. Karuppusamy and R.G. Saratale, *Microb. Pathog.*, **114**, 41 (2018); https://doi.org/10.1016/j.micpath.2017.11.013
7. A. Chatzigoulas, K. Karathanou, D. Dellis and Z. Cournia, *J. Chem. Inf. Model.*, **58**, 2380 (2018); https://doi.org/10.1021/acs.jcim.8b00269
8. K.V. Dorozhkin, G.E. Dunaevsky, S.Y. Sarkisov, V.I. Suslyaev, O.P. Tolbanov, V.A. Zhuravlev, Y.S. Sarkisov, V.L. Kuznetsov, S.I. Moseenkov, N.V. Semikolenova, V.A. Zakharov and V.V. Atuchin, *Mater. Res. Express*, **4**, 106201 (2017); https://doi.org/10.1088/2053-1591/aa8f06
9. M. Tharani, S. Rajeshkumar, K.A. Al-Ghanim, M. Nicoletti, N. Sachivkina and M. Govindarajan, *Biomedicines*, **11**, 1472 (2023); https://doi.org/10.3390/biomedicines11051472
10. V.M. Ankegowda, S.P. Kollur, S.K. Prasad, S. Pradeep, C. Dhramashekara, A.S. Jain, A. Prasad, C. Srinivasa, P.B. Sridhara Setty, S.M. Gopinath, R.P. S, A.H. Bahkali, A. Syed and C. Shivamallu, *Molecules*, **25**, 5042 (2020); https://doi.org/10.3390/molecules25215042
11. P. Reddy, S. Pradeep, S. M. Gopinath, C. Dharmashekar, G. Disha, M.T. Sai Chakith, C. Srinivasa, A.A. Shati, M.Y. Alfaifi, S.E.I. Elbehairi, R.R. Achar, E. Silina, V. Stupin, N. Manturova, C. Shivamallu and S.P. Kollur, *Front. Oncol.*, **13**, 1221275 (2023); https://doi.org/10.3389/fonc.2023.1221275
12. U. Ejaz, M. Afzal, M. Mazhar, M. Riaz, N. Ahmed, W.Y. Rizg, A.A. Alahmadi, M.Y. Badr, R.Y. Mushtaq and C.Y. Yean, *Int. J. Nanomed.*, **19**, 453 (2024); https://doi.org/10.2147/IJN.S446017
13. N.R. Farnsworth, *J. Pharm. Sci.*, **55**, 225 (1966); https://doi.org/10.1002/jps.2600550302
14. P. Velmurugan, K. Anbalagan, M. Manosathyadevan, K.-J. Lee, M. Cho, S.-M. Lee, J.-H. Park, S.-G. Oh, K.-S. Bang and B.-T. Oh, *Bioprocess Biosyst. Eng.*, **37**, 1935 (2014); https://doi.org/10.1007/s00449-014-1169-6
15. K.N. Prasad, B. Yang, J. Shi, C. Yu, M. Zhao, S. Xue and Y. Jiang, *J. Pharm. Biomed. Anal.*, **51**, 471 (2010); https://doi.org/10.1016/j.jpba.2009.02.033
16. 20 V.K. Sharma, R.A. Yngard and Y. Lin, *Adv. Colloid Interface Sci.*, **145**, 83 (2009); https://doi.org/10.1016/j.cis.2008.09.002
17. M.S. Kumar, S. Ethirajulu, G. Sethu, A.D. Raj, S.J. Sundaram, J.V. Kumar, M.W. Alam and P. Rosaiah, *Waste Biomass Valoriz.*, **15**, 5871 (2024); https://doi.org/10.1007/s12649-024-02578-1
18. E. Urnukhsaikhan, B.E. Bold, A. Gunbileg, N. Sukhbaatar and T. Mishig-Ochir, *Sci. Rep.*, **11**, 21047 (2021); https://doi.org/10.1038/s41598-021-00520-2
19. F.A. Cunha, K.R. Maia, E.J. Mallman, M.D. Cunha, A.A. Maciel, I.P. Souza, E.A. Menezes and P.B. Fechine, *Rev. Inst. Med. Trop.*, **58**, 73 (2016); https://doi.org/10.1590/S1678-9946201658073
20. W. Brand-Williams, M.E. Cuvelier and C.L.W.T. Berset, *Lebensm. Wiss. Technol.*, **28**, 25 (1995); https://doi.org/10.1016/S0023-6438(95)80008-5
21. F. Bothon, M. Atindéhou, Y. Koudoro, L. Lagnika and F. Avlessi, *Am. J. Plant Sci.*, **14**, 150 (2023); https://doi.org/10.4236/ajps.2023.142012
22. G.C. Yen and P.D. Duh, *J. Agric. Food Chem.*, **42**, 629 (1994); https://doi.org/10.1021/jf00039a005
23. P. Kakkar, B. Das and P.N. Viswanathan, *Indian J. Biochem. Biophys.*, **21**, 130 (1984).
24. M.T. Sultan, M.J. Anwar, M. Imran, I. Khalil, F. Saeed, S. Neelum, S.A. Alsagaby, W. Al Abdulmonem, M.A. Abdelgawad, M. Hussain, A.H. El-Ghorab, M. Umar and E. Al Jbawi, *Int. J. Food Prop.*, **26**, 526 (2023); https://doi.org/10.1080/10942912.2023.2166951
25. G. Tiwana, I.E. Cock and M.J. Cheesman, *Microorganisms*, **12**, 2664 (2024); https://doi.org/10.3390/microorganisms12122664
26. P. Khandel, S.K. Shahi, L. Kanwar, R.K. Yadaw, Ravi and D.K. Soni, *Int. J. Nano Dimen.*, **9**, 273 (2018).
27. M. Sastry, A. Ahmad, M. Khan and R. Kumar, *Curr. Sci.*, **85**, 162 (2003).
28. K. Jyoti, M. Baunthiyal and A. Singh, *J. Radiation Res. Appl. Sci.*, **9**, 217 (2016); https://doi.org/10.1016/j.jrras.2015.10.002
29. J. Ghilane, F.-R.F. Fan, A.J. Bard and N. Dunwoody, *Nano Lett.*, **7**, 1406 (2007); https://doi.org/10.1021/nl070268p
30. Z.H. Dhoondia and H. Chakraborty, *Nanomater. Nanotechnol.*, **2**, 15 (2012); https://doi.org/10.5772/55741

31. D.G. Jeung, M. Lee, S.M. Paek and J.M. Oh, *Nanomaterials*, **11**, 455 (2021); https://doi.org/10.3390/nano11020455
32. M.H. Ali, M.A.K. Azad, K.A. Khan, M.O. Rahman, U. Chakma and A. Kumer, *ACS Omega*, **8**, 28133 (2023); https://doi.org/10.1021/acsomega.3c01261
33. M. Goudarzi, N. Mir, M. Mousavi-Kamazani, S. Bagheri and M. Salavati-Niasari, *Sci. Rep.*, **6**, 32539 (2016); https://doi.org/10.1038/srep32539
34. M. Rai, A. Yadav and A. Gade, *Biotechnol. Adv.*, **27**, 76 (2009); https://doi.org/10.1016/j.biotechadv.2008.09.002
35. Q.L. Feng, J. Wu, G.Q. Chen, F.Z. Cui, T.N. Kim and J.O. Kim, *J. Biomed. Mater. Res.*, **52**, 662 (2000); https://doi.org/10.1002/1097-4636(20001215)52:4<662::AID-JBM10>3.0.CO;2-3
36. S. Ansar, H. Tabassum, N.S.M. Aladwan, M. Naiman Ali, B. Almaarik, S. AlMahrouqi, M. Abudawood, N. Banu and R. Alsubki, *Sci. Rep.*, **10**, 18564 (2020); https://doi.org/10.1038/s41598-020-74371-8
37. N. Konappa, A.C. Udayashankar, N. Dhamodaran, S. Krishnamurthy, S. Jagannath, F. Uzma, C.K. Pradeep, S. De Britto, S. Chowdappa and S. Jogaiah, *Biomolecules*, **11**, 535 (2021); https://doi.org/10.3390/biom11040535
38. L. Kvitek, A. Panacek, J. Soukupova, M. Kolar, R. Vecerova, R. Prucek, M. Holecová and R. Zboøil, *J. Phys. Chem. C*, **112**, 5825 (2008); https://doi.org/10.1021/jp711616v
39. Y.Y. Loo, Y. Rukayadi, M.-A.-R. Nor-Khaizura, C.H. Kuan, B.W. Chieng, M. Nishibuchi and S. Radu, *Front. Microbiol.*, **9**, 1555 (2018); https://doi.org/10.3389/fmicb.2018.01555
40. A. Ewunkem, T. Priester, D. Williams, B. Ariyon, I. Tshimanga, B. Justice and D. Singh, *J. Biomater. Nanobiotechnol.*, **15**, 51 (2024); https://doi.org/10.4236/jbnb.2024.153004
41. S. Seetharaman, V. Indra, B. Selva Muthu, A. Daisy and S. Geetha, *World J. Pharm. Pharm. Sci.*, **5**, 1328 (2016).
42. Y. Matsumura, K. Yoshikata, S. Kunisaki and T. Tsuchido, *Appl. Environ. Microbiol.*, **69**, 4278 (2003); https://doi.org/10.1128/AEM.69.7.4278-4281.2003
43. R. Vijayan, S. Joseph and B. Mathew, *Artif. Cells Nanomed. Biotechnol.*, **46**, 861 (2018); https://doi.org/10.1080/21691401.2017.1345930
44. X. Zhao, L. Zhou, M.S. Riaz Rajoka, L. Yan, C. Jiang, D. Shao, J. Zhu, J. Shi, Q. Huang, H. Yang and M. Jin, *Crit. Rev. Biotechnol.*, **38**, 817 (2018); https://doi.org/10.1080/07388551.2017.1414141
45. F. Cekic, S. Ekinci, M.S. Inal and D. Ünal, *Turk. J. Biol.*, **41**, 700 (2017); https://doi.org/10.3906/biy-1608-36
46. J. Yasur and P.U. Rani, *Environ. Sci. Pollut. Res. Int.*, **20**, 8636 (2013); https://doi.org/10.1007/s11356-013-1798-3
47. M. Velayutham, P. Sarkar, G. Sudhakaran, K.A. Al-Ghanim, S. Maboob, A. Juliet, A. Guru, S. Muthupandian and J. Arockiaraj, *Molecules*, **27**, 7333 (2022); https://doi.org/10.3390/molecules27217333
48. Y. Lee, H. Byun, J. Seok, K.A. Park, M. Won, W. Seo, S.-R. Lee, K. Kang, K.-C. Sohn, I.Y. Lee, H.-G. Kim, C.G. Son, H.-M. Shen and G.M. Hur, *Sci. Rep.*, **6**, 25094 (2016); https://doi.org/10.1038/srep25094
49. K. Satyavani, S. Gurudeeban, T. Ramanathan and T. Balasubramanian, *Avicenna J. Med. Biotechnol.*, **4**, 35 (2012).
50. P. Devaraj, P. Kumari, C. Aarti and A. Renganathan, *J. Nanotechnol.*, **2013**, 598328 (2013); https://doi.org/10.1155/2013/598328
51. S. Yeasmin, H.K. Datta, S. Chaudhuri, D. Malik and A. Bandyopadhyay, *J. Mol. Liq.*, **242**, 757 (2017); https://doi.org/10.1016/j.molliq.2017.06.047
52. R. Vijayan, S. Joseph and B. Mathew, *Artif. Cells Nanomed. Biotechnol.*, **46**, 861 (2018); https://doi.org/10.1080/21691401.2017.1345930